Low-temperature specific heats and magnetic properties of $Co_{100-x}Zr_x$ metallic glasses over a wide concentration range x=10-80

1989 J. Phys.: Condens. Matter 1 5903

(http://iopscience.iop.org/0953-8984/1/34/008)

J. Phys.: Condens. Matter 1 (1989) 5903–5913. Printed in the UK

Low-temperature specific heats and magnetic properties of $Co_{100-x}Zr_x$ metallic glasses over a wide concentration range $x = 10$–80

S Kanemaki†, O Takehira‡, K Fukamichi§ and U Mizutani‡

† Department of General Education, Nagoya University, Furo-cho, Chikusa-ku, Nagoya 464-01, Japan

‡ Department of Crystalline Materials Science, Nagoya University, Furo-cho, Chikusa-ku, Nagoya 464-01, Japan

§ Department of Materials Science, Tohoku University, Sendai 980, Japan

Received 17 February 1989

Abstract. $Co_{100-x}Zr_x$ metallic glasses were fabricated over a composition range $x = 10$–80 by using the ordinary liquid quenching technique in combination with the sputtering technique. A magnetic phase diagram is constructed through measurement of DC and AC magnetisation over the temperature range 4.2–800 K. Based on the magnetic phase diagram, we analysed the low-temperature specific heat data in the range 1.5–6 K and successfully singled out the contributions of electronic, lattice and magnetic specific heats. A spectrum of the electron density of states at the Fermi level over a whole Zr concentration range $x = 10$–80 has been deduced.

1. Introduction

The valence band structure of Zr–3d late transition metal M (M ≡ Fe, Co and Ni) binary metallic glasses has been studied through measurements of photoemission spectroscopy (Oelhafen *et al* 1980, Neddermeyer and Paul 1987) and low-temperature specific heats (Matsuura *et al* 1985, Matsuura and Mizutani 1986) as well as band calculations (Fairlie *et al* 1982, Moruzzi *et al* 1983). All these studies are consistent with the conclusion that the late transition metal forms its 3d band at higher binding energies and the host metal Zr forms its 4d band at the Fermi level E_F, resulting in a split-band structure with two separate d-peaks.

A number of experimental studies have been already reported in Zr-rich Zr–M binary metallic glasses. Included, for example, are the measurements of magnetic susceptibility, Hall coefficient (Altounian and Strom-Olsen 1983, Flodin *et al* 1986, Trudeau *et al* 1988) and superconductivity (Karkut and Hake 1983). More recently, Kanemaki *et al* (1988b) reported the Zr concentration-dependence of the low-temperature specific heats, magnetic susceptibilities and the electrical resistivities in all three metallic glasses Fe–Zr, Co–Zr and Ni–Zr and pointed out that magnetic states characteristic of the respective alloy systems substantially affect the observed electronic properties. Among these three, the concentration dependence of various electronic properties in the Fe–Zr alloy system has been the most thoroughly studied, since

0953-8984/89/345903 + 11 $02.50

amorphous single phase samples were fabricated over a wide composition range, 8–80 at.% Zr, with the use of the ordinary liquid quenching technique in combination with the sputtering technique (Matsuura *et al* 1985).

Co–Zr metallic glasses, on which the present studies focus, are non-magnetic and exhibit superconductivity in the Zr–rich composition range, whereas they become ferromagnetic when the Zr concentration is reduced below 40 at.% (Heiman and Kazama 1978). Stobiecki *et al* (1987) prepared Co–Zr metallic glass samples over the range 10–84 at.% Zr by the sputtering technique and revealed that the Hall coefficient changes its sign from negative to positive, when the Zr content exceeds about 50 at.%. It is of great interest to study in greater detail the magnetic effect on various electronic properties across the whole composition range in the Co–Zr metallic glass system. Using the ordinary liquid quenching technique in combination with the sputtering, we were able to prepare metallic glasses over the composition range 10–80 at.% Zr in the alloy system Co–Zr. We report the results on the magnetic properties in the temperature range 4.2–800 K and on the low-temperature specific heats in the range 1.5–6 K. Discussion is focused on the Zr concentration-dependence of the low-temperature specific heats with reference to the magnetic states deduced from magnetic measurements.

2. Experimental procedure

Co–Zr alloy ingots were prepared by arc-melting appropriate amounts of 99.9% Co and 99.5% Zr in a high-purity argon atmosphere. Ribbon samples, about 1 mm wide and 15 μm thick, were obtained for $Co_{100-x}Zr_x$ alloys with $x = 10, 15, 45, 50, 60, 70$ and 80, using a single-roll spinning wheel apparatus in a reduced Ar gas atmosphere. Samples with $x = 20, 30, 40$ and 50 were prepared by sputtering the respective alloys onto a Cu substrate. The sputtering was continued over 72 h, resulting in samples of thickness about 0.6 mm and diameter about 45 mm. The deposit was later removed by mechanical polishing. All samples were confirmed to be fully amorphous by x-ray diffraction measurements using Cu Kα radiation.

Low-temperature specific heats were measured in the temperature range 1.5–6 K, using a sample of weight 2–3 g, which was compacted in a Cu container. The ordinary adiabatic method was employed, the details of which are described elsewhere (Massalski and Mizutani 1978). The specific heats of the 50 at.% Zr alloy were measured on both liquid-quenched ribbons and sputtered plates. No serious difference was detected within the accuracy of the measurements, confirming that the results are independent of the method of sample preparation. Both magnetisation and magnetic susceptibility were measured in a DC field of 1 T in the temperature range 4.2–800 K. The AC magnetic susceptibility was also measured in a field strength of 10 Oe ($= (10^4/4\pi)$ A m^{-1}) at 80 Hz in the range 4.2–300 K for two metallic glasses, $Co_{70}Zr_{30}$ and $Co_{60}Zr_{40}$. The mass density was also measured for Co-rich sputtered samples by Archimedes' method, using xylene as a working fluid.

3. Results

3.1. Magnetic properties

A spontaneous magnetisation has been observed up to 30 at.% Zr. The Curie temperature T_C is determined from its temperature dependence only for the alloys with $x =$

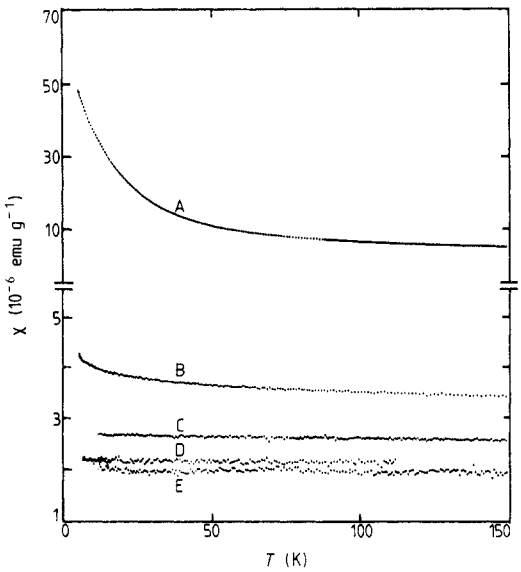

Figure 1. Temperature dependence of the magnetic susceptibility in the range 4.2–150 K for $Co_{100-x}Zr_x$ metallic glasses. Curve A, $x = 40$; curve B, $x = 45$; curve C, $x = 50$; curve D, $x = 60$; curve E, $x = 70$.

20 and 30. The Curie temperature for the alloys with $x = 10$ and 15 could not be determined because of its rise beyond the crystallisation temperature. The spinwave stiffness constant was deduced by fitting the magnetisation curve measured under the magnetic field of 1 T to the expression

$$M(T)/M(0) = 1 - BT^{3/2} - CT^{5/2} \tag{1}$$

where $M(T)$ and $M(0)$ are the magnetisation at T and 0 K, respectively, and B and C are fitting parameters. The coefficient B is related to the spinwave stiffness constant D through the equation

$$B = [2.61g\mu_B/M(0)](k_B/4\pi D)^{3/2} \tag{2}$$

where g is the g-factor, μ_B is the Bohr magneton and k_B is the Boltzmann constant.

The DC magnetic susceptibility data are shown in figure 1 for alloys in the composition range $40 \leqslant x \leqslant 70$. The Curie–Weiss-type temperature dependence is evident for alloys with $x = 40$ and 45. The magnetic susceptibility for the 50 at.% Zr sputtered alloy still exhibits a finite negative slope, though its curvature is negligibly small. However, its temperature dependence is almost completely lost when the Zr content exceeds 60 at.%. The AC magnetic susceptibility measurement on the 40 at.% Zr sample revealed the absence of any cusp or anomaly down to 4.2 K, indicating that no magnetic order appears to take place.

The superconducting transition temperature T_{sc} has been observed for alloys containing more than 53 at.% Zr (Altounian and Strom-Olsen 1983). Based on the present magnetic data, we constructed in figure 2 the magnetic phase diagram, in which the value of T_{sc} is incorporated. As is clearly visible, the ferromagnetism continues up to almost 40 at.% Zr and the temperature-dependent paramagnetism appears down to the lowest temperatures in the range 40–50 at.% Zr. The spin-glass region, if it exists, should be located in the range centred around 35 at.% Zr.

Relevant numerical data in this section are listed in table 1.

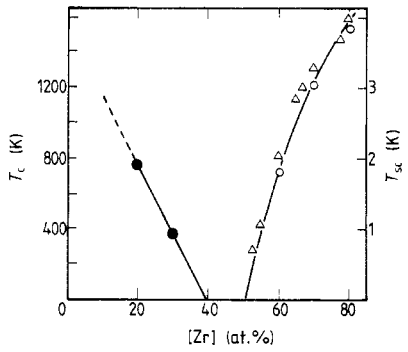

Figure 2. ●, the Curie temperature T_C and, ○, △, the superconducting transition temperature T_{sc} for the Co–Zr metallic glasses. ○, T_{sc} derived from the present low-temperature specific heat measurements; △, data derived from the resistivity measurements by Altounian and Strom-Olsen (1983).

Table 1. Magnetic properties of Co–Zr metallic glasses. R and S refer to samples prepared by liquid quenching in the form of ribbons and by sputtering, respectively. The value of the spin-wave specific heat coefficient σ_{sw} is deduced from the spin-wave stiffness constant D through equation (4) (see text).

[Zr] (at.%)	Form	T_C (K)	μ (μ_B/Co atom)	D (meV A^2)	d (g cm^{-3})	σ_{sw} (mJ mol^{-1} K)$^{-5/2}$	H_{int} (kOe)
10	R	—	1.51	370	—	0.0401	207
15	R	—	1.31	315	—	0.0532	161
20	S	750	1.19	262	8.28	0.0738	147
30	S	370	0.75	133	8.14	0.216	134
40	S	—	—	—	7.86	—	—

3.2. *Low-temperature specific heat*

The low temperature specific heat data are shown in the form of C/T against T^2 in figure 3 (*a*), (*b*) and (*c*) for alloys with different Zr contents 10–30, 40–50 and 60–80 at.%, respectively. The low-temperature specific heat in the ferromagnetic regime $x = 10$–30 is characterised by a small upturn at low temperatures. The data in ferromagnetic Co-rich alloys should be analysed in terms of the expression

$$C = \gamma T + \alpha T^3 + \sigma_{sw} T^{3/2} + \sigma_n T^{-2} \tag{3}$$

where γ is the electronic specific heat coefficient, α is the lattice specific heat coefficient, from which the Debye temperature θ_D is derived, σ_{sw} is the spin-wave specific heat coefficient and σ_n the nuclear specific heat coefficient. The nuclear specific heat arises from the interaction of ^{59}Co nuclei with the internal magnetic field H_{int}. The term σ_{sw} contributes to the downward deviation in the C/T versus T^2 plot, whereas the term σ_n contributes to the upward deviation with decreasing temperature. An observed upturn implies that the nuclear specific heat contribution supersedes that of the spin-wave term. This does not necessarily mean that the spin-wave contribution is negligibly small. We estimated the value of σ_{sw} independently from the temperature dependence of magnetisation or the spin wave stiffness constant D through the relation

$$\sigma_{sw} = 39.431(W/d)D^{-3/2} \tag{4}$$

where σ_{sw} is in mJ mol^{-1} K$^{-5/2}$, W is the average atomic weight in g and d is the measured

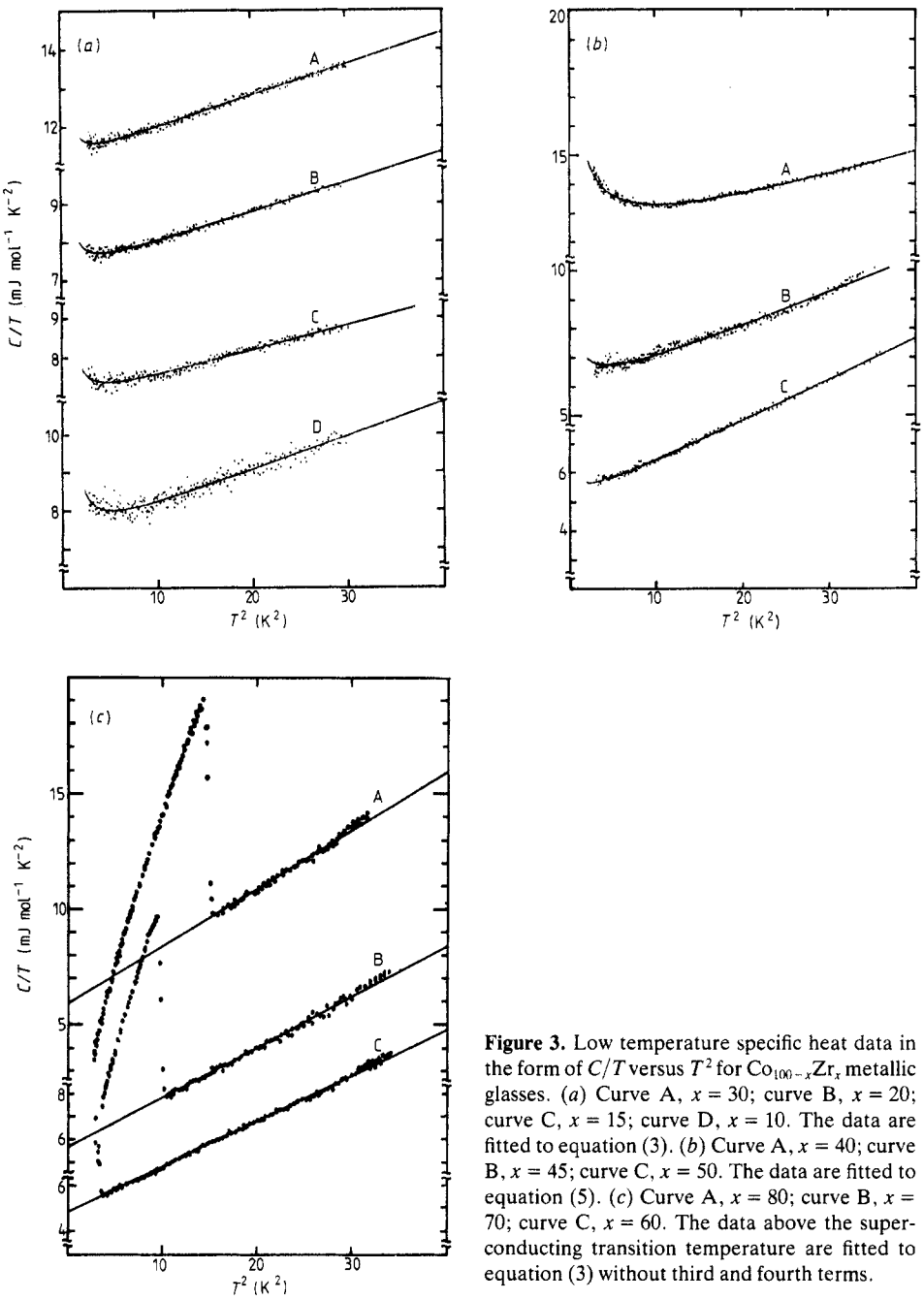

Figure 3. Low temperature specific heat data in the form of C/T versus T^2 for $Co_{100-x}Zr_x$ metallic glasses. (*a*) Curve A, $x = 30$; curve B, $x = 20$; curve C, $x = 15$; curve D, $x = 10$. The data are fitted to equation (3). (*b*) Curve A, $x = 40$; curve B, $x = 45$; curve C, $x = 50$. The data are fitted to equation (5). (*c*) Curve A, $x = 80$; curve B, $x = 70$; curve C, $x = 60$. The data above the superconducting transition temperature are fitted to equation (3) without third and fourth terms.

mass density in g cm^{-3}. Once the value of σ_{sw} is given, the remaining three coefficients in equation (3) can be reliably determined by least-squares fitting.

The contribution of the nuclear specific heat naturally decreases with decreasing Co concentration and diminishes, in principle, when the ferromagnetism disappears. The low-temperature specific heat data for the 40–50 at.% Zr samples shown in figure 3(*b*)

also exhibit the upturn at low temperatures. They are no longer ferromagnetic and, instead, the magnetic state is described by the temperature-dependent paramagnetism. The low-temperature specific heat data for the alloys in this family are fitted to the equation

$$C = \gamma T + \alpha T^3 + A \tag{5}$$

where A is assumed to represent the magnetic specific heat in the temperature range 1.5–6 K, where the measurements were made. The coefficient A is believed to represent the magnetic specific heat well, when the magnetic inhomogeneities are appreciable (Mizutani and Hasegawa 1988).

All specific heat data shown in figure 3(*c*) exhibit a jump at low temperatures owing to the onset of superconductivity. The low-temperature specific heat data in the normal state can be well expressed by the sum of the first and second terms in equation (3). All numerical coefficients thus determined are listed in table 2.

4. Discussion

4.1. Electronic specific heat

The measured electronic specific heat coefficient γ_{exp} is plotted in figure 4 as a function of Zr concentration. It is clear from figure 4 that the value of γ_{exp} peaks sharply at about 40 at.% Zr, where the ferromagnetism breaks down. It is well known that the linearly temperature-dependent magnetic specific heat γ_{mag} superimposes onto the ordinary band structure contribution γ_{band} in the composition range where ferromagnetism is unstable. Apparently, the present results indicate that the term γ_{mag} exists in the composition range $20 \leqslant x \leqslant 45$.

Apart from the region where γ_{mag} is apparently finite, the value of γ_{exp} is considered to reflect the band-structure contribution γ_{band}, particularly if the electron–phonon enhancement can be properly corrected for. The enhancement factor λ for superconducting alloys with $x = 60$, 70 and 80 can be estimated from the McMillan formula (1968)

$$\lambda = [1.04 + \mu \ln(\theta_D/1.45T_{sc})]/[(1-0.62\mu)\ln(\theta_D/1.45T_{sc}) - 1.04] \tag{6}$$

where μ is the Coulomb repulsive constant and is taken as 0.13 for the present alloys. The value of λ is also calculated for metallic glasses with 53 and 55 at.% Zr, for which the superconducting transition temperature is available in the literature (Altounian and Strom-Olsen 1983). The value of λ for Co–Zr metallic glasses is plotted in figure 5. The value of γ_{band}, obtained by dividing the measured value by $(1 + \lambda)$, is plotted in figure 4 as full circles. Here the data for the 50 at.% Zr alloy are treated on the same footing, although the magnetic susceptibility showed a weak temperature dependence.

The electron–phonon enhancement effect for the Co-rich ferromagnetic alloys cannot be evaluated quantitatively because of the absence of superconductivity. For the sake of simplicity, we temporarily assume that the value of λ is 0.3 for alloys with $x = 10$ and 15, for which γ_{mag} is believed to be negligible. The resulting γ_{band} values are shown in figure 4 and connected smoothly with the values for alloys containing more than 50 at.% Zr.

The curve passing through all values of γ_{band} is believed to represent the overall band-structure profile across the whole Zr concentration range. The density of states at

Table 2. Low-temperature specific heat data for Co–Zr metallic glasses. R and S refer to samples prepared by liquid quenching in the form of ribbons and by sputtering, respectively.

[Zr] (at.%)	Form	γ (mJ mol^{-1} K^{-2})	α (mJ mol^{-1} K^{-4})	θ_D (K)	σ_n (mJ K mol^{-1})	A (mJ mol^{-1} K^{-1})	T_{sc} (K)	λ
10	R	7.17 ± 0.03	0.0894 ± 0.0012	279 ± 1	3.86 ± 0.31	—	—	0.3
15	R	6.78 ± 0.02	0.0637 ± 0.0007	312 ± 1	2.19 ± 0.18	—	—	0.3
20	S	7.10 ± 0.01	0.0769 ± 0.0006	293 ± 1	1.73 ± 0.13	—	—	—
30	S	8.83 ± 0.01	0.0765 ± 0.0006	294 ± 1	1.26 ± 0.15	—	—	—
40	S	10.6 ± 0.1	0.0914 ± 0.0006	277 ± 1	—	5.73 ± 0.07	—	—
45	R	5.99 ± 0.05	0.0987 ± 0.0012	270 ± 1	—	0.57 ± 0.11	—	—
50	S	4.76 ± 0.04	0.144 ± 0.001	238 ± 1	—	0.86 ± 0.09	—	0.4
60	R	4.85 ± 0.06	0.199 ± 0.003	214 ± 1	—	—	1.8	0.54
70	R	5.68 ± 0.02	0.219 ± 0.001	207 ± 1	—	—	3.04	0.62
80	R	5.93 ± 0.04	0.251 ± 0.002	198 ± 1	—	—	3.83	0.67

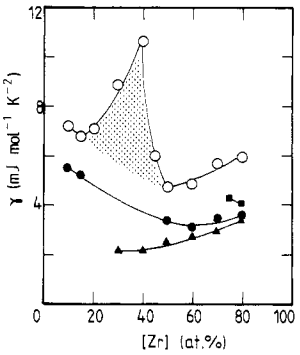

Figure 4. The measured γ_{exp} value for the Co–Zr metallic glasses. ○, data. The band structure contribution γ_{band} are shown for the M–Zr (M ≡ Fe, Co and Ni) metallic glasses: ●, Co–Zr; ■, Fe–Zr (Matsuura *et al* 1985; ▲, Ni–Zr (Matsuura and Mizutani 1986).

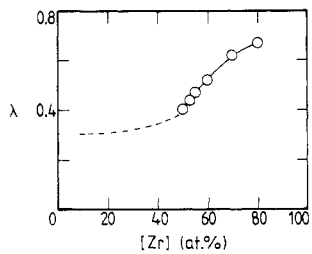

Figure 5. The electron–phonon enhancement factor λ for the Co–Zr metallic glasses. The value is calculated from the McMillan formula at the composition where the experimental T_{sc} or θ_D values are available (see figure 2).

the Fermi level decreases up to 60 at.% Zr and, then, turns to increase in higher Zr concentration range. A triangular-shaped region bounded by the γ_{exp} and $(1 + \lambda)\gamma_{band}$ represents the linearly-temperature-dependent magnetic specific heat coefficient γ_{mag}.

The composition dependence of γ_{band} has been already deduced in the same manner as above for the Zr-rich Fe–Zr (Matsuura *et al* 1985) and Ni–Zr (Matsuura and Mizutani 1986) metallic glasses. The results are incorporated in figure 4. It is clear that the value of γ_{band} in both Co–Zr and Ni–Zr alloy systems initially decreases almost linearly with decreasing Zr content and that the reversal of the slope occurs at 60 and 40 at.% Zr in the Co–Zr and Ni–Zr systems, respectively. We consider that an 'upward deviation' already begins at 75 at.% Zr in the Fe–Zr alloy system without an initial decrease. It must also be noted that the value of γ_{band} is at its highest in Fe–Zr, intermediate in Co–Zr and lowest in Ni–Zr.

According to the photo-emission studies and band calculations for the Zr-rich Zr–M (M ≡ Fe, Co and Ni) metallic glasses, the 3d-band of Fe appears closest to the Fermi level, whereas that of Ni is farthest and well-separated from the Zr 4d-states near E_F. The location of the Co 3d-band in the Zr-rich Co–Zr metallic glasses is in between these two cases (Oelhafen *et al* 1980). Hence, the closer the 3d-band relative to E_F, the higher the value of γ_{band}. This naturally explains why the value of γ_{band} increases in the order Ni, Co and Fe for a given Zr concentration. An initially decreasing trend of γ_{band} with decreasing Zr content in both Co–Zr and Ni–Zr can be interpreted as a decrease in the Zr 4d-states at E_F. Here the contribution of the 3d-band located at higher binding energies is insignificant.

When Zr content is reduced, however, the 3d-band of the late transition metal grows and moves gradually towards E_F. As a result, its contribution to γ_{band} eventually

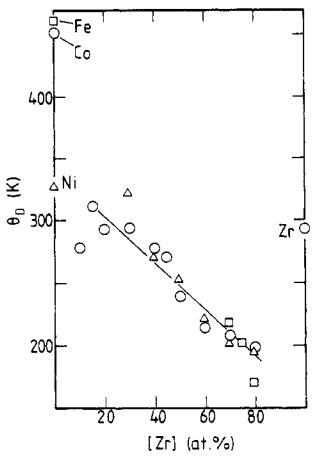

Figure 6. The Debye temperature θ_D: ○, Co–Zr metallic glasses; □, Fe–Zr (Matsuura *et al* 1985), △, Ni–Zr (Matsuura and Mizutani 1986). The Debye temperatures for the pure elements Zr, Co, Ni and Fe are also included.

supersedes that of the Zr 4d-states and causes an upward deviation of the otherwise linearly decreasing γ_{band}. The value of γ_{band} increases more-or-less linearly with further decrease in Zr content. We consider that not only the growth of the Co 3d-band but also its movement towards the Fermi level should be responsible for the rather sharp increase in γ_{band} and also for the occurrence of the ferromagnetism in the Co-rich region. The value of γ_{band} for the ferromagnetic alloys with $x = 10$ and 15 exceeds 5 mJ mol^{-1} K^{-2}. Such a high value of γ_{band} is typical of a metallic glass, for which the Fermi level is located in the middle of the d-band. From which we conclude that the electronic structure for the ferromagnetic Co-rich metallic glasses is characterised by the possession of the Fermi level in the Co 3d-band.

4.2. Lattice specific heat

Figure 6 shows the Zr concentration dependence of the Debye temperature θ_D for the Co–Zr metallic glasses in the present work, together with the data for Fe–Zr (Matsuura *et al* 1985) and Ni–Zr (Matsuura and Mizutani 1986). The value of θ_D decreases almost linearly with increasing Zr content, regardless of the atomic species of the alloying partners Fe, Co and Ni. The value is also found to be much smaller than that for pure elements Zr, Co and Fe. The crystallisation temperature T_x in these M–Zr metallic glasses has been reported to decrease with increasing Zr, in the manner similar to the Debye temperature mentioned above (Buschow and Beekmans 1979). Their results are reproduced in figure 7(*a*), along with the melting temperature T_m for pure Zr, Co and Ni.

The interrelation between the T_x and θ_D has been discussed in relation to the Lindemann melting formula (Matsuura and Mizutani 1986, Kanemaki *et al* 1988a)

$$x_m = (3\hbar/\theta_D)(T_x/Mk_B)^{1/2}(4\pi/3V_a)^{1/3} \tag{7}$$

where x_m is the ratio of the RMS displacement of atoms to the mean atomic radius, M is the average atomic mass and V_a is the volume per atom. The value of x_m is considered to reflect the critical amplitude of the atomic vibrations, beyond which the amorphous phase is no longer stable. The value of x_m for pure elements is also calculated by inserting into equation (7) the melting temperature T_m in place of T_x. As shown in figure 7(*b*), the resulting value of x_m is around 0.18, regardless of whether the amorphous phase

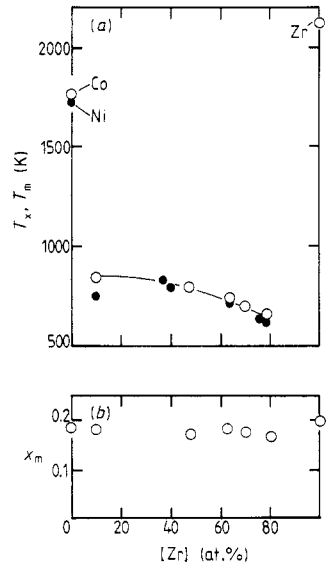

Figure 7. (*a*) Crystallisation temperature T_x, ○, for Co–Zr, and ●, Ni–Zr metallic glasses obtained by Buschow and Beekmans (1979). Melting temperatures T_m for the pure elements Zr, Co and Ni are also included. (*b*) Ratio of the RMS displacement to the mean atomic radius x_m for Co–Zr metallic glasses and pure Zr and Co metals.

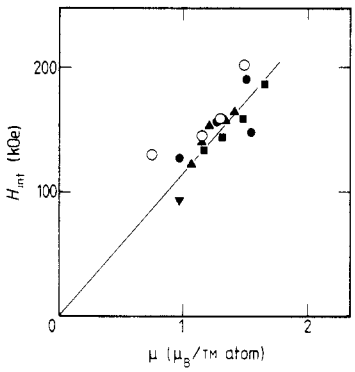

Figure 8. Internal magnetic field H_{int} against the average magnetic moment per 3d-transition metal atom in various Co-based metallic glasses. ○, Co–Zr (present work); ●, Co–Y (Mizutani *et al* 1987); ■, $(Fe–Co)_{77}B_{13}Si_{10}$ (Mizutani and Takeuchi 1986); ▼, $(Co–Ni)_{77}B_{13}Si_{10}$ (Mizutani and Takeuchi 1986); ▲, Co–B (Matsuura and Mizutani 1983).

crystallises or the crystal melts. This implies that the crystallisation temperature plays basically the same role as the melting temperature in the crystalline state and that the relatively low Debye temperature in the amorphous phase reflects a substantial difference between T_x and T_m.

4.3. Magnetic specific heat

We briefly discuss the nuclear magnetic specific heat arising from the ^{59}Co nuclei interacting with the internal field. The nuclear magnetic specific heat coefficient σ_n can be expressed in terms of the internal magnetic field H_{int} by

$$\sigma_n = xR[(I+1)/3I](4.583\mu_n H_{int}/k_B)^2 \tag{8}$$

where μ_n is the nuclear magneton, I the nuclear spin of $\frac{7}{2}$ for ^{59}Co nuclei and x the fraction of Co atoms. The internal magnetic field obtained by inserting the measured σ_n into equation (8) is plotted in figure 8 as a function of the average magnetic moment per 3d-transition metal (TM) atom for various Co-based metallic glasses (present work,

Matsuura and Mizutani 1983, Mizutani and Takeuchi 1986, Mizutani *et al* 1987). It can be seen that all data fall on a straight line passing through zero. From this we conclude that the internal field is proportional to the average magnetic moment per atom, irrespective of the non-magnetic partner element involved.

Acknowledgment

The authors are grateful to Professor T Goto, University of Tokyo, for providing us with the opportunity to use the DC and AC magnetic susceptibility equipment in the Institute for Solid State Physics.

References

Altounian Z and Strom-Olsen J O 1983 *Phys. Rev.* B **27** 4149
Buschow K H J and Beekmans N M 1979 *Phys. Rev.* B **19** 3843
Fairlie R H, Temmerman W M and Gyorffy B L 1982 *J. Phys. F: Met. Phys.* **12** 1641
Flodin M, Hedman L and Rapp Ö 1986 *Phys. Rev.* B **34** 4558
Heiman N and Kazama N 1978 *Phys. Rev.* B **17** 2215
Kanemaki S, Suzuki M, Yamada Y and Mizutani U 1988a *J. Phys. F: Met. Phys.* **18** 105
Kanemaki S, Takehira O and Mizutani U 1988b *Trans. Japan Inst. Met. Suppl.* **29** 347
Karkut M G and Hake R R 1983 *Phys. Rev.* B **28** 1396
Massalski T B and Mizutani U 1978 *Prog. Mater. Sci.* **22** 151
Matsuura M and Mizutani U 1983 *J. Phys. F: Met. Phys.* **13** 1539
Matsuura M and Mizutani U 1986 *J. Phys. F: Met. Phys.* **16** L183
Matsuura M, Mizutani U and Fukamichi K 1985 *Proc. 5th Int. Conf. Rapidly Quenched Metals (Würzburg)* ed. S Steeb and H Warlimont (Amsterdam: Elsevier) p 1019–22
McMillan W L 1968 *Phys. Rev.* **167** 331
Mizutani U, Fukamichi K and Goto T 1987 *J. Phys. F: Met. Phys.* **17** 257
Mizutani U and Hasegawa M 1988 *Physica* B **149** 267
Mizutani U and Takeuchi M 1986 *J. Phys. F: Met. Phys.* **16** 79
Moruzzi V L, Oelhafen P, Williams A R, Lapka R Güntherodt H-J and Kübler J 1983 *Phys. Rev.* B **27** 2049
Neddermeyer H and Paul Th 1987 *Phys. Rev.* B **36** 4148
Oelhafen P, Hauser E and Güntherodt H-J 1980 *Solid State Commun.* **35** 1017
Stobiecki T, Bayreuther G and Hoffmann H 1987 *Magnetic Properties of Amorphous Metals* ed. A Hernando, V Madurga, M C Sánchez-Trujillo and M Vázquez (Amsterdam: Elsevier) p 188–90
Trudeau M L, Cochrane R W and Destry J 1988 *Mater. Sci. Eng.* **99** 187